STRUCTURES AND ENERGETICS OF BICYCLIC ORGANIC MOLECULES USING PHOTOELECTRON SPECTROSCOPY

by

Sydney Cordova

A Thesis Submitted to the Faculty of the

DEPARTMENT OF CHEMISTRY AND BIOCHEMISTRY

In Partial Fulfillment of the Requirements

For the Degree of

MASTER OF SCIENCE

In the Graduate College

THE UNIVERSITY OF ARIZONA

2025

THE UNIVERSITY OF ARIZONA
GRADUATE COLLEGE

As members of the Master's Committee, we certify that we have read the thesis prepared by Sydney Cordova, titled *Structures and Energetics of Bicyclic Organic Molecules using Photoelectron Spectroscopy* and recommend that it be accepted as fulfilling the dissertation requirement for the Master's Degree.

Dr. Andrei Sanov — Date: 12/3/25

Dr. Thomas Purcell — Date: 12/3/25

Dr. Steve Schwartz — Date: 12/3/25

Final approval and acceptance of this thesis is contingent upon the candidate's submission of the final copies of the thesis to the Graduate College.

I hereby certify that I have read this thesis prepared under my direction and recommend that it be accepted as fulfilling the Master's requirement.

Dr. Andrei Sanov — Date: 12/3/25
Master's Thesis Committee Chair
Department of Chemistry and Biochemistry

Table of Contents

List of Figures

Abstract:

Organic molecules are important in chemistry and relevant to many applications. The bicyclic molecules of anthranil, 1,2-benzisoxazole, and benzoxazole are all made from a benzene ring and a five-membered ring containing a nitrogen and oxygen atoms. They are often used as scaffolds in medicinal chemistry and drug design. However, despite their notable use in synthesis, not much is known about the energetics of these molecules. Using photoelectron spectroscopy, the adiabatic electron affinities of anthranilyl and 1,2-benzisoxazolyl were measured. Anthranilyl has two distinct states, nearly overlapping electronic adiabatic electronic affinities of 3.12 eV and 3.34 eV, while for 1,2-benzisoxazolyl only one state is observed around 2.94 eV. The completion of these experiments allows for a broader comparison to be made between the isomer family and the five-membered rings. Combined with previous work done for the other three molecules, the effect that location of the heteroatoms has on the energies and electronic structures of the radical states can be analyzed. The results indicate that anthranilyl has the largest EA of the bicyclic isomers and the addition of the benzene ring causes additional π-stabilization. The similarities in the behaviors between the bicyclic rings and the five-membered rings show that the addition of the benzene does not always have a large effect. This work brings light to the relationship between molecules in an isomer family and the effect that moving the heteroatoms can have.

Chapter 1: Introduction

1.1 - Importance of organic bicyclic molecules

Bicyclic molecules are often used in medicinal chemistry and drug design as a starting element in the process of creating new drugs. A question to answer is what physical elements are sought after in a starting molecule and what the biological application of a finished drug can be. Ring systems are analyzed for physicochemical, structural and electronic properties to understand and overcome specific problems, such as synthetic limitations and molecule stability.[1] Here, 1,2-benzisoxazole and 2,1-benzisoxazole (anthranil) will be discussed in depth, leading to a comparison between them and the third bicyclic isomer benzoxazole, which has been studied previously.[2]

These bicyclic molecules consist of a five-membered ring, oxazole or isoxazole, fused to a benzene ring.[3] Bicyclic molecules of this size are quite common and are important as they occur naturally and can be seen as strong test-beds for physical organic phenomena.[4] The inclusion of the nitrogen and oxygen atoms are two important elements of great interest in starting molecules for drug design.[5] Two of these isomers have successfully been used in drugs that are available on the market.[6, 7] Benzisoxazoles have been called some of the most important building blocks in drug design.[7] The benzene ring allows for several additions to create diverse molecules, but can be utilized in a ring open form which can allow for substitutions of different heteroatoms. Benzisoxazole (Bix) and benzoxazole (Bzox) are often intact in the final, larger synthesized drugs. Anthranil (Ant) is often exploited as an intermediate, or an accidental molecule produced along a synthetic pathway and has the least number of developed drugs on the market.[8, 9]

There have been studies focused on the aromaticity of these molecules and the behavior of those elements.[3, 10, 11] Anthranil behaves similar to naphthalene, with its aromaticity centered in the five-membered ring. The other two isomers, benzisoxazole and benzoxazole, have the aromaticity centered within the benzene ring. This can be beneficial as that balance being adjacent to the oxazole or isoxazole rings can introduce favorable interactions.[6] While aromaticity is not a large factor in this study, it plays a role in understanding the stability and reactivity of the molecules. It can influence how rings rehybridize or reconjugate to gain stability after deprotonation.[12, 13]

There are clear differences and similarities when looking at the structures of these three isomers. With the lack of information known about them, these studies look into the energies involving the anion and neutral radical forms. These forms allow for studying the electronic structures and analyzing how the carbons in the benzene rings aid stabilization of the deprotonated structures. While the information discussed here may not be directly relevant towards medicinal chemistry, it adds to the general knowledge of these molecules and to the dialogue surrounding bicyclic molecules.

1.2 – Photoelectron spectroscopy

Photoelectron spectroscopy relies on the photoelectric effect which relates the binding energy of the electrons and the energy of the incident light to find the electron kinetic energy. Photodetachment of negative ions, in conjunction with the spectrum from the corresponding neutral molecules, facilitates the understanding of the quantum mechanics of chemical bonding of the neutral radical and electronic structure of the anions. An anion in a ground electronic and vibrational state is excited by absorbing a photon and detaching an electron, leaving the corresponding neutral radical in a higher electronic and vibrational state. The analytical method

uses the equation below where the photoemitted electron's kinetic energy (eKE) is found by the energy of the photon from a light (hv) source minus the electron's binding energy. The incident light source, like a laser, is used to photoeject the electron.[14]

$$\text{eKE} = h\nu - \text{eBE} \tag{1.1}$$

Those photoejected electrons reach hundreds of thousands of iterations and as they hit the detector, the photoelectron image is obtained. The analysis of that image produces the photoelectron spectrum. Within the spectrum, electronic and vibrational peaks are seen with their respective intensities controlled by the Franck-Condon (FC) Principle. Specifically, the intensity of a vibrational peak from an allowed electronic transition between the anion and neutral states due to the absorption of a photon is proportional to the square of the corresponding FC integral, defined as

$$FCF = \langle \psi_{final} | \psi_{initial} \rangle = \langle \psi_{f,nuc} | \psi_{i,nuc} \rangle \langle \psi_{f,el} | \hat{\mu} | \psi_{i,el} \rangle \tag{1.2}$$

where ψ_{nuc} represents the nuclear vibrational wavefunctions of the initial (anion) and final (neutral) states. ψ_{el} represents the corresponding electronic wavefunctions for those states with the dipole operator ($\hat{\mu}$) term dependent only on those components. The FC principle is based on the Born-Oppenheimer Approximation, as the nuclei are stated to be in a fixed position relative to their fast-moving electrons. The neutral molecule is assumed to have the same geometry as the anion when the electron is photoejected, producing the vertical detachment energy (VDE).

The VDE usually corresponds to the most intense peak in the spectrum, reflecting the detachment of the vibrational state of the neutral with the greatest Franck-Condon overlap to the vibrational ground state of the anion. This approximation neglects the eKE dependence on the electronic part of the photodetachment cross-section. It can also help predict the stability of the

anion states. This is different from the adiabatic electron affinity (EA), where the ground vibrational level of the anion corresponds to the ground vibrational state in the neutral. The VDE tends to be a higher value than the EA due to the assumption of the geometry not changing.

1.3 – Thesis outline

In this thesis, Chapter 2 outlines the basics of the experimental instrumentation and broad experiment parameters. From there, it will discuss the five molecules whose structures are shown in Figure 1. Chapter 3 discusses the first molecule studied 2,1-benzisoxzole or anthranil. The electron affinity and other energetic properties were determined and are highlighted for both a σ and π radical states of the neutral molecule. The next chapter will discuss the second isomer, 1,2-benzisoxazole and the ongoing analysis that is being done to understand the spectrum and theory. Lastly, Chapter 5 introduces the previously studied molecules benzoxazole, oxazole, and isoxazole which are labeled **3**, **4**, and **5** within the figure below respectively. The content of these experiments is summarized so that a comprehensive comparison of the three bicyclic isomers and their five-membered rings can be made. The comparisons are outlined using the arrows in the figure below. The electron affinities will be compared as well as the influence that the location of the C-H bond, relative to the heteroatoms, has on those values and the molecular behavior.

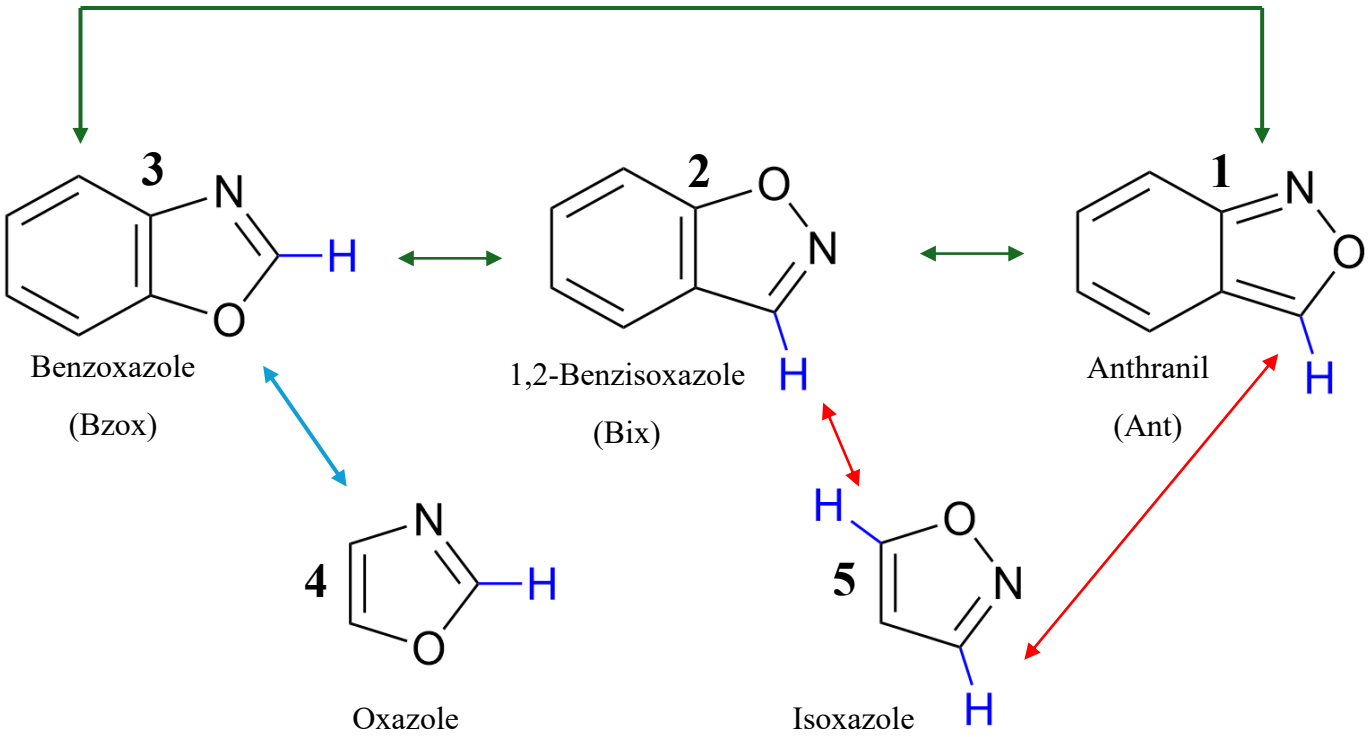

Figure 1: Structures of the molecules mentioned in this thesis and the pathways for the comparisons between the 5 molecules. The color of the arrows represents the different comparisons that will be discussed.

Chapter 2: Instrumentation Details

The experiments that are discussed here were performed on instrumentation that has been described previously.[15, 16] In this section important elements of the instrumentation are highlighted. To introduce the sample into the source chamber, a carrier gas at varying pressures mixes with the sample, creating a vapor. That mixture gets introduced to the chamber and is pulsed through a supersonic nozzle operating at either 50 Hz or 20 Hz to match the repetition rate of the laser system used.

The electron source used in the new detailed experiments is the electron cannon configuration.[14, 17, 18] It is similar to an electron gun configuration, a design commonly used in many photoelectron spectroscopy studies. The cannon is essentially the gun without the optical elements. The cannon set-up provides a wider spray of electrons, increasing its area and creating more ions than the use of an electron gun would. Electrons are sprayed to interact with the sample mixture coming through the nozzle, where the impact creates the large number of anions that are essential to these experiments.

Within the cannon, there is a thoria-coated iridium filament which is kept at -100 V to -400 V, depending on the experiment and is heated by a direct current of ~5 A. As the ion beam travels forward in the chamber, it interacts with a metal plate that is pulsed down to about -700 V to -900 V, sending the beam into the flight tube of the Wiley-McLaren[19] time-of-flight mass spectrometer.[20] This allows for a representative mass spectrum to be formed. As the ions continue through the instrument, they are intersected by a laser beam for photodetachment. There are two laser systems used in these studies. The first is a Spectra Physics Lab-130-50 Nd:YAG laser operating at a repetition rate of 50 Hz, utilizing different harmonics to achieve different wavelengths. The other is a Continuum Surelite II-20 Nd:YAG laser operating at 20 Hz.

The resulting photodetached electrons were analyzed using a velocity-map imaging (VMI)[21] assembly described elsewhere.[15] The three VMI electrodes were kept at varying voltages and projected the electrons in a direction perpendicular to the ion and laser beams. The three electrodes are kept at negative, neutral and positive voltages from bottom to top respectfully. The electrons are then detected by a 40 mm diameter dual microchannel plate detector coupled to a P47 phosphor screen (Burle Inc.).[22] The images are captured using a CCD camera.

The resulting photoelectron images are analyzed using published procedures[23, 24] and the BASEX program[25] is used to create the inverse Abel[26] transformed images. Any experiment specific settings will be described in the respective chapters in further detail.

Chapter 3: Photoelectron spectroscopic study of Anthranil (2,1-Benzisoxazole)

3.1- Molecule background

2,1-benzisoxazole, commonly known as anthranil, is an isoxazole ring bonded to a benzene ring (molecule **1** in Figure 1). Due to where the rings fuse together, the double bonds in the isoxazole force a change in the benzene ring, converting it into a cyclohexadiene form. Anthranil has been used in medicinal chemistry and drug design for biological applications such as MAO inhibitors[27] and anticonvulsants.[9] In synthesis, anthranil is not often used as a starting component, but rather synthesized along the pathway as an intermediate. In finished products, it does not remain in its traditional structure as some atoms get may substituted or bonds may be broken since anthranil is a rich molecule for C-H bonds and C-N bonds.[8, 28]

3.2 – Experimental environment

A small sample of anthranil (brown-reddish liquid; Santa Cruz Biotechnology, 99%) at room temperature was raised to an elevated position in the sample holder. This was done to invite easier vaporization with a carrier gas of O_2 at ~1.56 atm. The experiment was done at 355 nm using the Continuum Surelite II-20 Nd:YAG laser at a repetition rate of 20 Hz. The three VMI electrodes were kept at -165 V, 0 V, and +450 V, respectively as the laser polarization direction is in the plane.

3.3- Experimental results

The photoelectron images were collected at 355 nm (3.495 eV). The raw and Abel transformed images are shown in Figure 2 and used to produce the photoelectron spectrum using BASEX programs. The spectrum is plotted as intensity with respect to the eBE in electron volts, determined by equation 1.1 which allows for the identification of the adiabatic electron affinity.

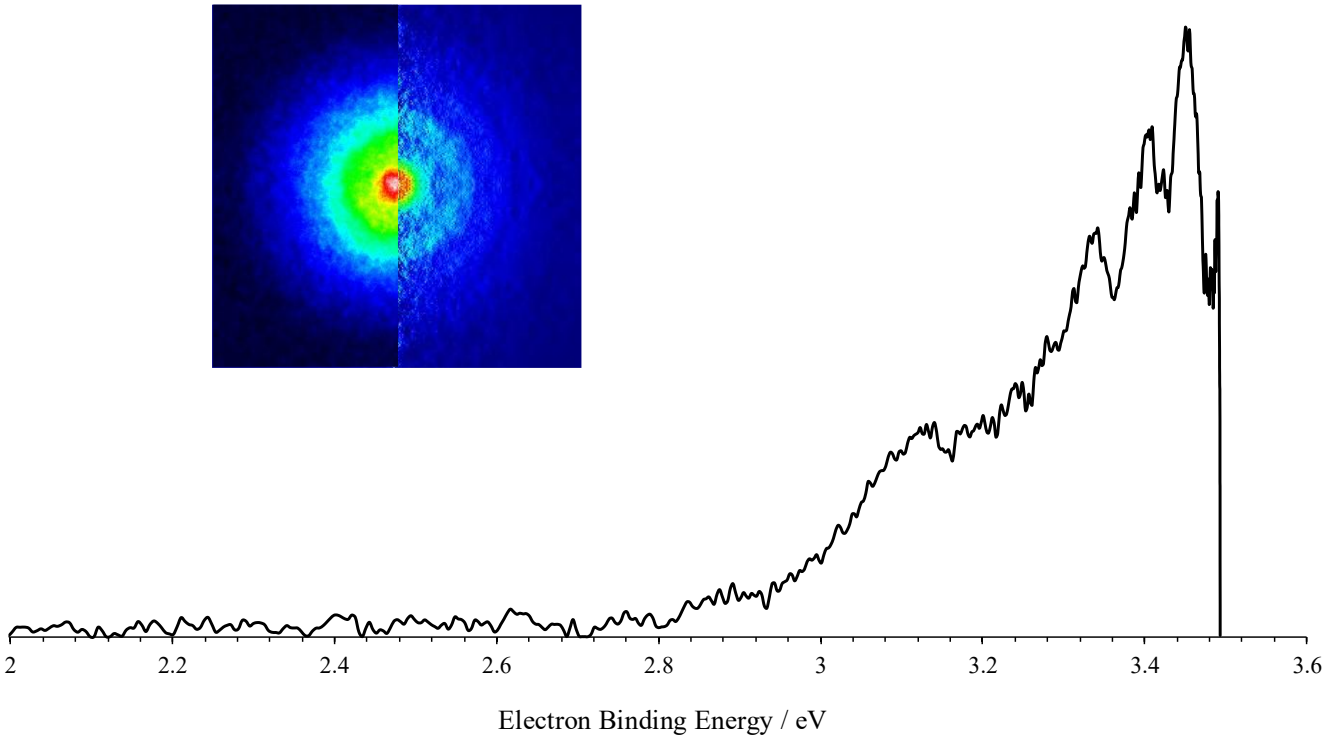

Figure 2: Photoelectron images and spectrum of C3-anthranide. The raw (left) and inverse Abel transformation images (right) captured at 355 nm.

3.4 – Theoretical detail

There are five locations for potential deprotonation within this molecule and to confirm which C-H bond was deprotonated, geometry optimization calculations were done using wB97X-D/aug-cc-pVDZ level theory. The results showed that the C3 site, which is the carbon in the 5-membered ring near the oxygen atom, is the most stable site for deprotonation. As shown in Figure 3, the C3 isomer is the only site with a resulting theoretical EA that falls within the discernable area of the spectrum. From the optimized geometry results, it was noted that there could be more than one radical isomer produced from this location. For verification, optimization was done using B3LYP level of theory which determined that both a σ and π radical is possible from deprotonation at this site. In these studies, the labels σ and π are used colloquially to describe electronic states of A′ and A″ symmetry, respectively. Both radical states stay in a ring-closed confirmation, and the resulting energies show that the π-isomer may be at a lower energy than the σ.

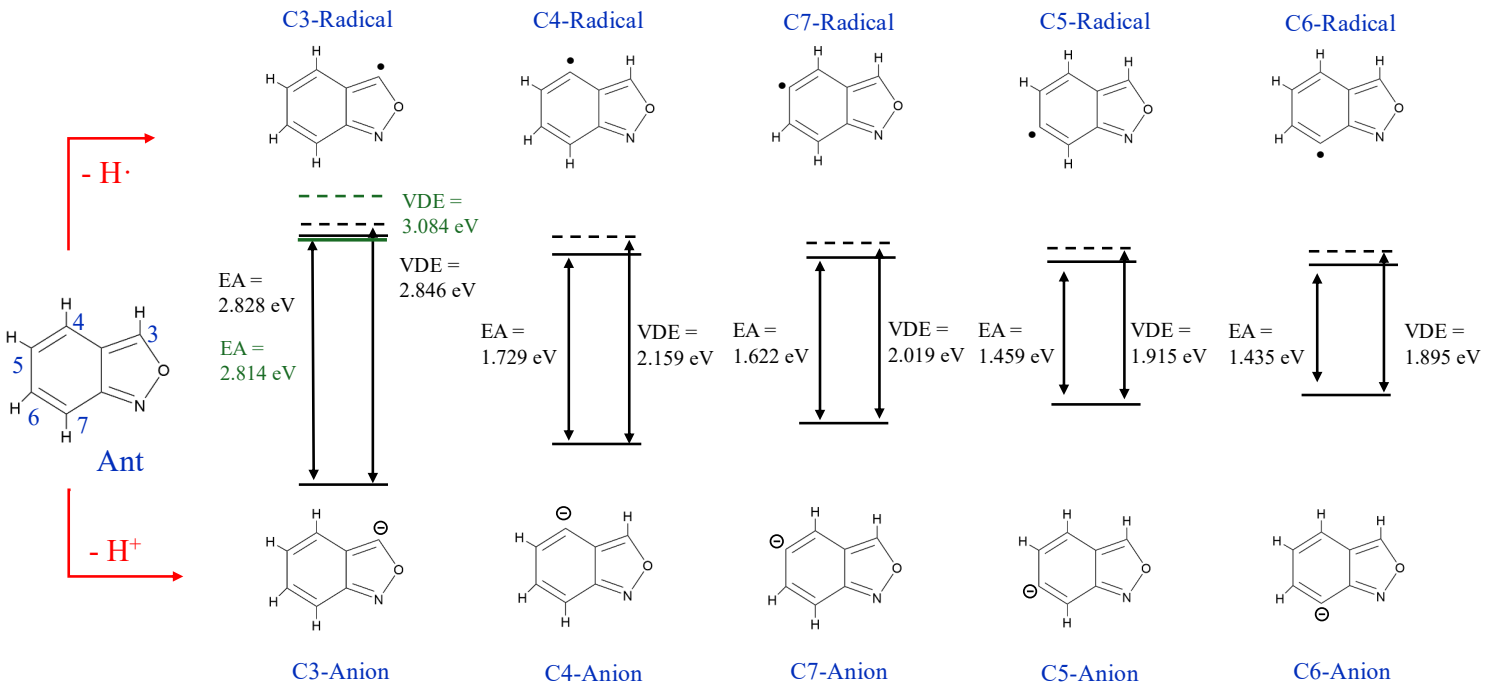

Figure 3: Theoretical electron affinities and vertical detachment energies for C-H deprotonation pathways in anthranil calculated at wB97X-D/aug-cc-pVDZ level theory. The C3 energy values are B3LYP/aug-cc-pVDZ level. All representations are in the σ state, and the green lines represent the C3 π-state.

To confirm if and where in the spectrum each respective isomer was, an EOM-IP-CCSD calculation was done. This couple cluster (CCSD) calculation with ionization potential (IP) equation-of-motion (EOM)[29] determines the respective radical energies of the optimized geometries by removing either an A′ or A″ electron from the reference geometry. This calculation confirmed that there were two conformations within the spectrum and gave values for where in the spectrum they appear. The theory results showed that π radical was calculated at 3.014 eV and the σ radical at 3.338 eV. The values from the EOM-IP calculations are used to adjust the FC spectra to better fit the characteristics of the experimental spectrum.

The Franck-Condon factors[30-32] from the frequencies done at the lower level of theory for the radical and anion were calculated using QChem 5.1[33] licensed to the Sanov group using B3LYP/aug-cc-pVDZ level theory. This analysis includes Dushinsky rotations[34] of the normal modes which relied on the geometries and harmonic vibrational frequencies. These factors are used to produce the theoretical spectra that is then modeled using MATLAB. The two spectra produced are: one red, which has a narrow broadening function that depicts the vibrational transitions, and one blue, which is mixed with a broader Gaussian function to represent the electronic, vibrational transitions. These two spectra are modeled alongside the experimental spectrum in Figure 4. Within the spectrum, the π-isomer is responsible for the first peak at 3.12 eV and the σ-isomer contributes to the higher energy peaks in the spectrum with the main peak being around 3.34 eV.

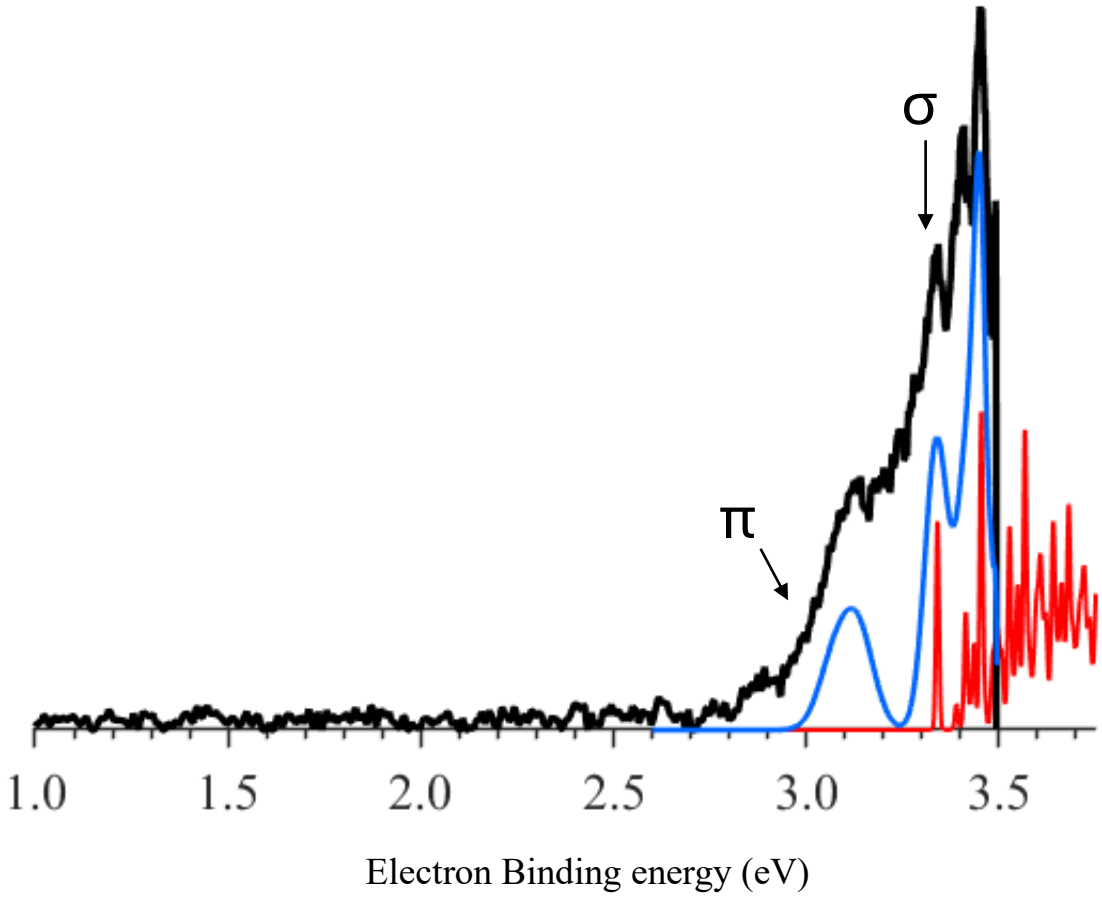

Figure 4*:* Photoelectron spectrum of anthranil combined with the Franck-Condon simulations. The black line is the experimental spectrum, the red is a FC spectrum presenting the vibrational transitions, and blue is a FC spectrum showing an electronic vibrational spectrum. The peaks are labeled to highlight the locations of the two different isomers**.**

3.5 – Discussion of results

The π isomer being at a lower energy than the σ is due to the benzene ring acting as a π-stabilizing force as the additional carbons stabilize the charge and the imbalance from the photodetachment.[12] The π isomer does not have as large of an influence in the experimental spectrum as the σ isomer, which is reflected in the FC spectra as the σ isomer is responsible for both peaks at the higher energies. The π isomer is responsible for the first peak, which is at a lower intensity, in the spectrum as seen in Figure 4.

The aromaticity of this molecule is centered in the isoxazole ring due to the placement of the double bonds, and π-electrons, within the molecule.[3, 10] This balance of aromaticity is what allows for the ring to stay closed in either deprotonated form as it strengthens the N-O bond. Furthermore, the lone pairs on the oxygen atom relocating into the deprotonated orbitals when an A″ electron is removed from the molecule is what allows for the π-state to be stable at the lower energy.[13]

Calculations showed that both the π radical and the σ radical stay closed rings at optimized geometries. The VDE determined at the lower-level theory for the π radical is 3.083 eV, about a 0.27 eV difference to the theoretical EA showing that the geometry of the radical may have a large difference from the anion. The σ radical has a smaller theoretical VDE but the modeled FC spectrum depicts that it is responsible for both peaks at the higher end of the spectrum. The largest peak around 3.43 eV may represent the VDE for this isomer, meaning there is about a 0.1 eV difference in value. Figure 5 shows the CCSD optimized geometries for the anions and radicals overlaid for ease of comparison with respect to bond lengths and angles. The largest differences are the N-O bond length and the angle of the deprotonated carbon. The σ isomer has the largest angle at the C3 position and the shortest N-O bond. These geometry

changes support the broader peaks that the sigma isomer has within the photoelectron spectrum. The trend seen in the values of the π isomer supports the similarity in geometry to the anion as it has a much smaller influence on the spectrum as well as a lack of a vibrational element of the FC spectra. The increase in N-O bond length could predict where the bond would break if the system were to become ring open.

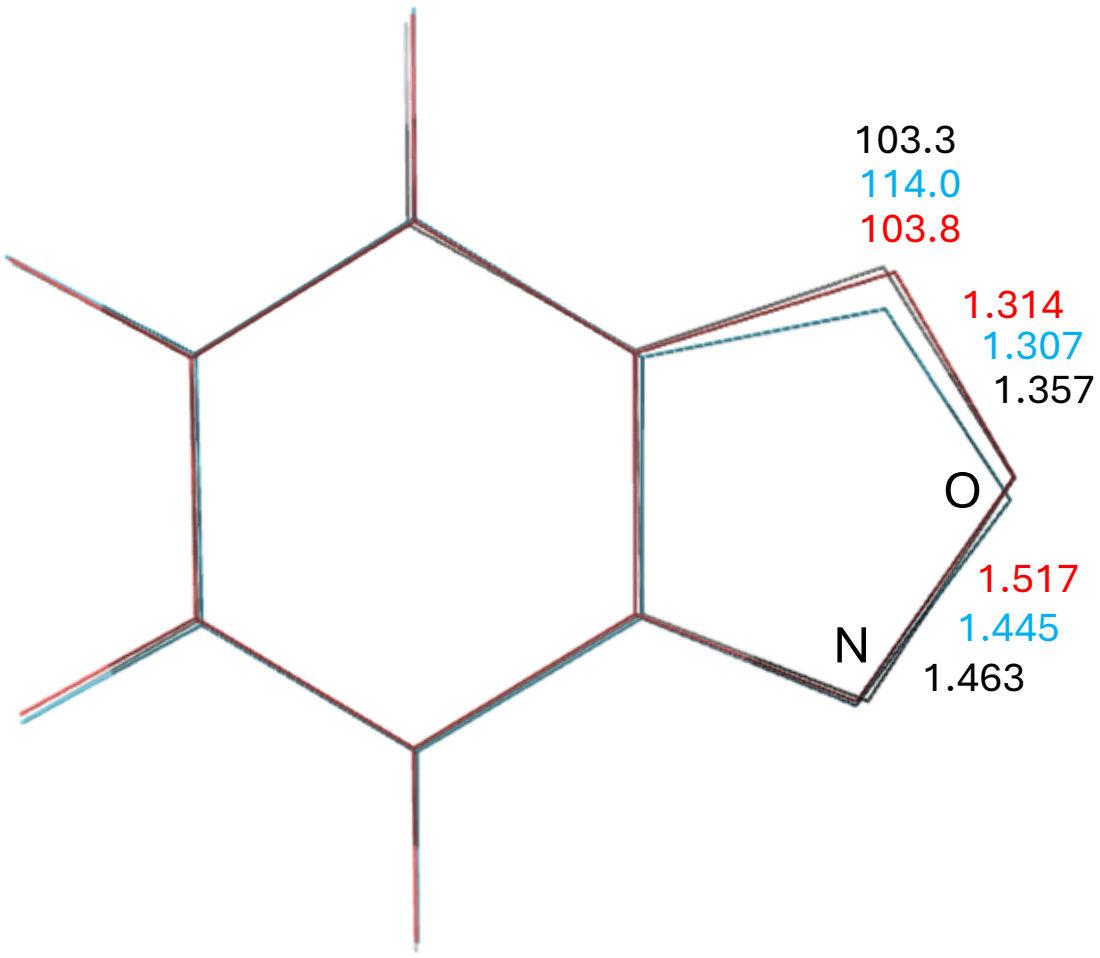

Figure 5: Wire frame representations of the optimized anion state (black) layered with the σ-Ant (blue) and π-Ant (red) radicals at CCSD/aug-cc-pVDZ. The bond lengths are reported in angstroms.

3.6 – Summary

The deprotonation of anthranil results in two radical isomers present in the photoelectron spectrum. The most stable site of deprotonation is the C3 next to the oxygen atom in the five-membered ring. The two radicals are a σ-radical and a π-radical. The π radical lies at a lower energy value of 3.12 eV while the σ radical is towards the higher end of the spectrum at 3.34 eV. The σ isomer has large geometrical differences from the anion while the π isomer is geometrically similar.

Chapter 4: Analyzing 1,2-Benzisoxazole Using Photoelectron Imaging

4.1 – Importance

1,2-benzisoxazole (benzisoxazole) is composed of a benzene ring and isoxazole ring, bonded at the 4,5 carbons of the isoxazole ring (molecule **2**). Bonding here allows the benzene ring to stay in a traditional conformation and it remains in its full form in the finished drugs, where it is often functionalized at the C3 carbon on the five-membered ring.[5] This molecule has been proven to be biologically active in different types of drugs like anti-inflammatory agents, antipsychotics and many more, with several drugs that use this scaffold are available on the market.[7, 35]

4.2 – Experimental environment

A sample of ~1 mL was placed in the sample holder and is lifted to a position that creates direct contact between the carrier gas and the sample. A carrier gas of O_2 at a pressure of 0.34 atm was used to vaporize the sample and flow into the source chamber. This experiment was done at 355 nm using a Spectra-Physics Lab-130-50 Nd:YAG laser at a repetition rate at 50 Hz, using the third harmonics. It was repeated using 1.10 atm O_2 and 355 nm light from the Continuum Surelite II-20 Nd:YAG at a repetition rate at 20 Hz to verify the experiment. Both experiments were achieved with the VMI electrodes at -330 V, 0 V and +900 V, respectively.

4.3 – Experimental results

The images were collected at 355 nm (3.495 eV) laser light. The corresponding photoelectron spectrum was made using BASEX and graphed on an axis of intensity versus the eBE. Figure 6 shows both photoelectron spectra side by side; the left spectrum is from the original experiment and the right from the repeated experiment.

A.

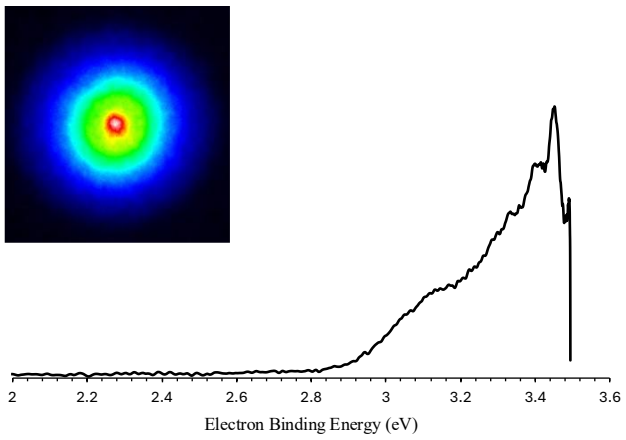

B.

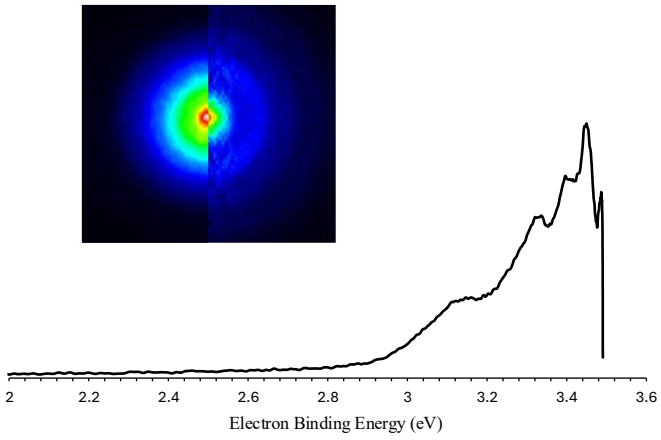

Figure 6: The photoelectron spectrums of 1,2-benzisoxazole produced from the respective obtained photos to the left of each at 355 nm. Spectrum A is from the original experiment, and B is from the repeated experiment.

To determine which carbon was deprotonated, calculations at wM97X-D/aug-cc-pVDZ level theory were done. Figure 7 shows that the C3 carbon can be the only location responsible for the spectrum since the theoretical EA values of the other C-H sites are too low to appear within the discernable bounds of the spectrum. These initial calculations indicated that the ring would open at the optimized geometry for both the radical and the anion. While not clearly seen in the spectrum, this is supported further by calculations done at CCSD/aug-cc-pVDZ level of theory.

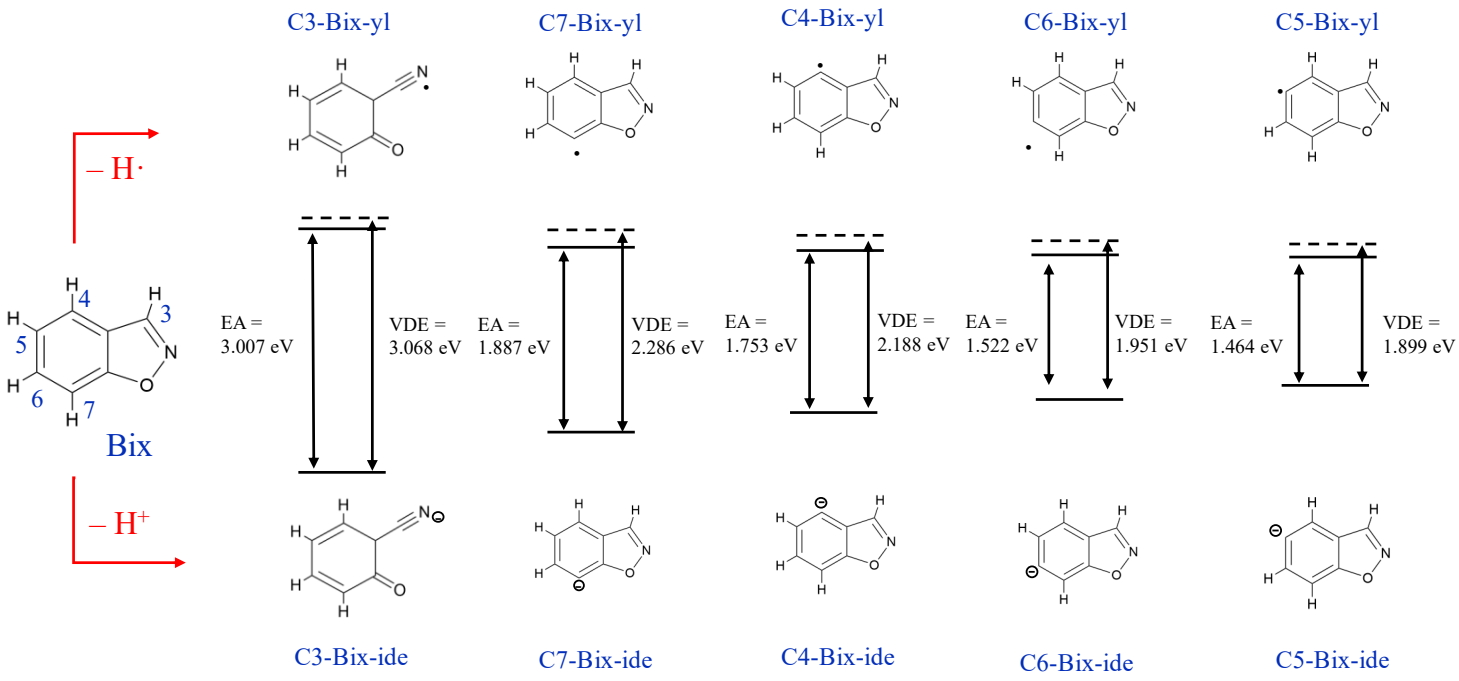

Figure 7: Theoretical electron affinities and vertical detachment energies for C-H bond dissociation pathways calculated using wB97X-D/aug-cc-pVDZ level theory for 1,2-benzisoxazole.

To model the experimental spectrum with theoretical models, the Franck-Condon factors were determined using the lower-level theory results. The produced spectrum did not fit well with the experimental spectrum, so different approaches were taken by using varied parameters to simulate different FC factors.

One hypothesis is that the spectrum may be produced from 'hot ions' so the temperature was raised to 700 K from 0 K. As well, the vibrational excitations for the anion (initial) state and radical (target) state with respect to the Duschinsky rotations were changed. The pairings that were done include 0:6, 0:8, 1:6, and 2:6 for the anion and radical respectively. This did not lead to a definitive answer, so an EOM-IP-CCSD calculation was done. In this calculation, two electrons were deprotonated at both the A′ or A″ levels to estimate the EA for the two lowest energy levels. The resulting values lead to the conclusion that only one isomer, the lowest π isomer at 2.941 eV, is within the range of the photoelectron spectrum.

4.4 – Discussion of results

Due to the continuing confusion, the experiment was redone at similar settings to confirm the experimental spectrum. The resulting spectrum is nearly identical to the original one but has more defined characteristics. One parameter that is confirmed from the FC simulations is that there are no hot ions present. At this stage of analysis, many of the spectra calculated at 0 K can model the π isomer within the discernable bounds using 2.94 eV to fit the spectrum. This isomer appears at an early point in the spectrum, most likely aligning with the band peal. However, the model could not be accurately fit to the experimental spectrum due to the data not being in agreement.

The computations confirm that at either the wB97X-D or CCSD level of theory, the ring will open. This ring opens, unlike its isomers, due to its aromaticity and bond strength. The aromaticity within the molecule is focused within the benzene ring more than the isoxazole ring, making the N-O bond weak.[10] When the C3 is deprotonated the ring opens and rearranges to regain stability, and the nitrogen forms a triple bond with the neighboring carbon.[36] This ring opening supports other literature findings[37], but the photoelectron spectrum does not model a ring-open molecule. This change is shown in the optimized geometries presented in Figure 8. Further investigation will need to be done to determine where the inconsistencies may lie.

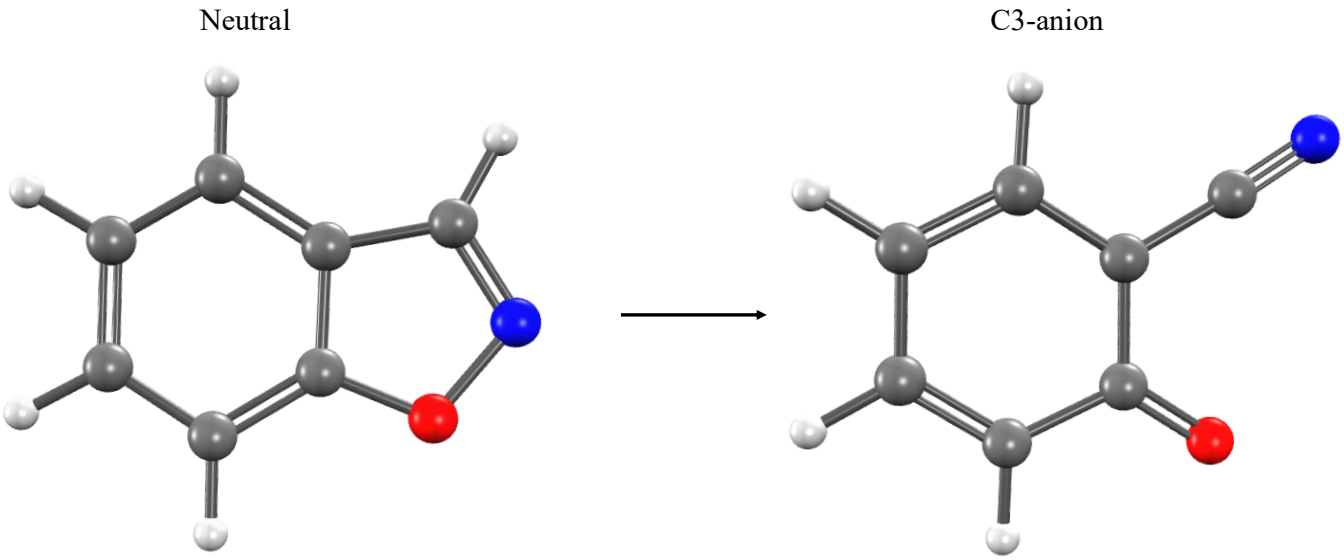

Figure 8: Ball and stick models of the optimized CCSD level of theory geometry of the neutral and anion form of C3-1,2-benzisoxazole.

4.5 – Summary

The experimental spectrum developed from the photoelectron image of benzisoxazole looks very similar to that of anthranil, but the molecule does not appear to behave the same. From calculations, the lowest π radical level should fall within the spectrum around 2.941 eV, but the theoretical results do not agree with the experimental spectrum. There will need to be further work done to try and understand why the calculations result in a ring-opening, but the experimental spectrum does not show that.

Chapter 5: Comparisons

5.1 – Previously Studied Molecules

To compare the isomer family to each other, the previously studied molecules need to be detailed. These studies were done using the same methods and instrumentation. While these studies may have been done at multiple wavelengths, only the data obtained from 355 nm will be discussed.

5.1.1 – Benzoxazole

The first molecule to discuss is benzoxazole, the third bicyclic isomer of the group (molecule **3**).[2] This experiment was done using 355 nm light from the Spectra Physics Lab Nd:YAG laser, using O_2 as the carrier gas at a pressure of 1.4 atm. After producing the photoelectron spectrum seen in Figure 9, it was determined that the ground state radical (σ-BzOx-yl) yielded an electron affinity of 2.75 eV when deprotonated at the C2 location. This is the lowest transition allowed without the molecule becoming a ring-open anion or radical. This confirmed that the photoelectron spectrum only includes one isomer. The electronic structure of the isomer showed that the angle between the N-C-O bonds changes, resulting in the radical having a smaller angle and bond lengths than the anion form. It is worth nothing that it is possible for the molecule to form a ring-open anion. Its corresponding neutral would contribute to a narrow peak early in the spectrum, but it cannot be easily separated from the first peak.

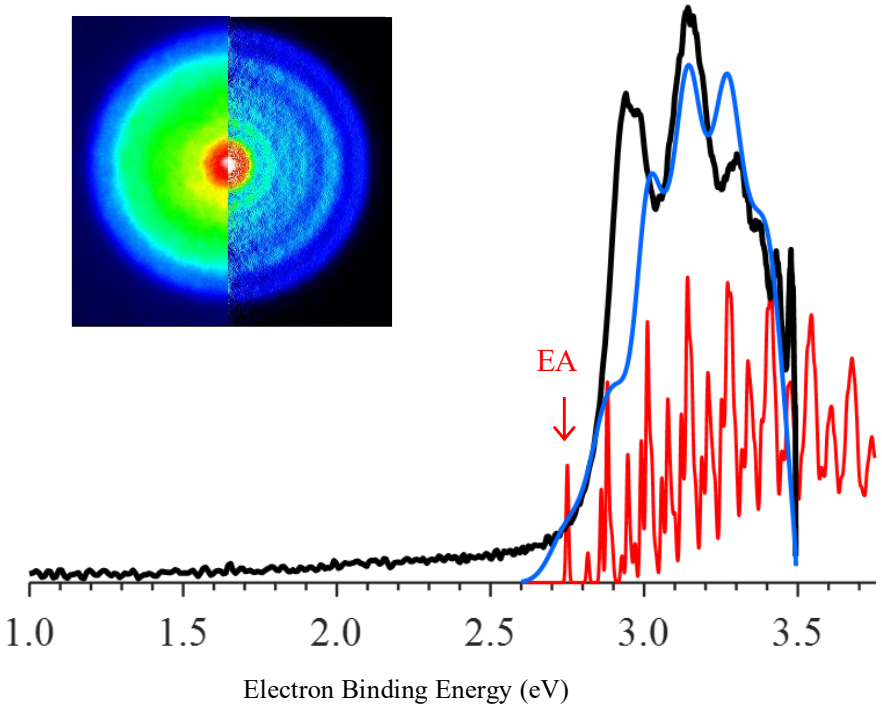

Figure 9: Photoelectron images and spectrum of benzoxazole. The image is composed of the raw (left) and inverse Abel transformed data (right). The black line is the experimental spectrum, and the others are from the FC factors based on the calculations done using B3LYP/aug-cc-pVDZ level of theory. The figure is based on data from reference 2.

5.1.2 – Oxazole

The next molecule to discuss is oxazole (**4**). This is one of the two five-membered rings included in these bicyclic molecules. The study done by Culberson, et al.[38] was focused on the C2-oxazolide anion and corresponding neutral radical. This was achieved by selective deprotonation, allowing for the C2 site to be the primary deprotonation site. 2-D-oxazole was synthesized then analyzed using argon gas at 30 psi. The incident light was from the Spectra Physics Nd:YAG laser, with the acceleration electrodes at -330 V, 0 V, and 900 V respectively. The resulting spectrum from the 355 nm light was partially resolved, so a Franck-Condon simulation was done at B3LYP/6-31+G* level of theory to help clarify the band peak as seen in Figure 10. The resulting adiabatic electron affinity was found to be 2.21 eV for the neutral radical. When comparing the anion and neutral electronic structures, the angle between the O-C-N bonds was larger in the neutral radical compared to the anion while the bond lengths were shorter.

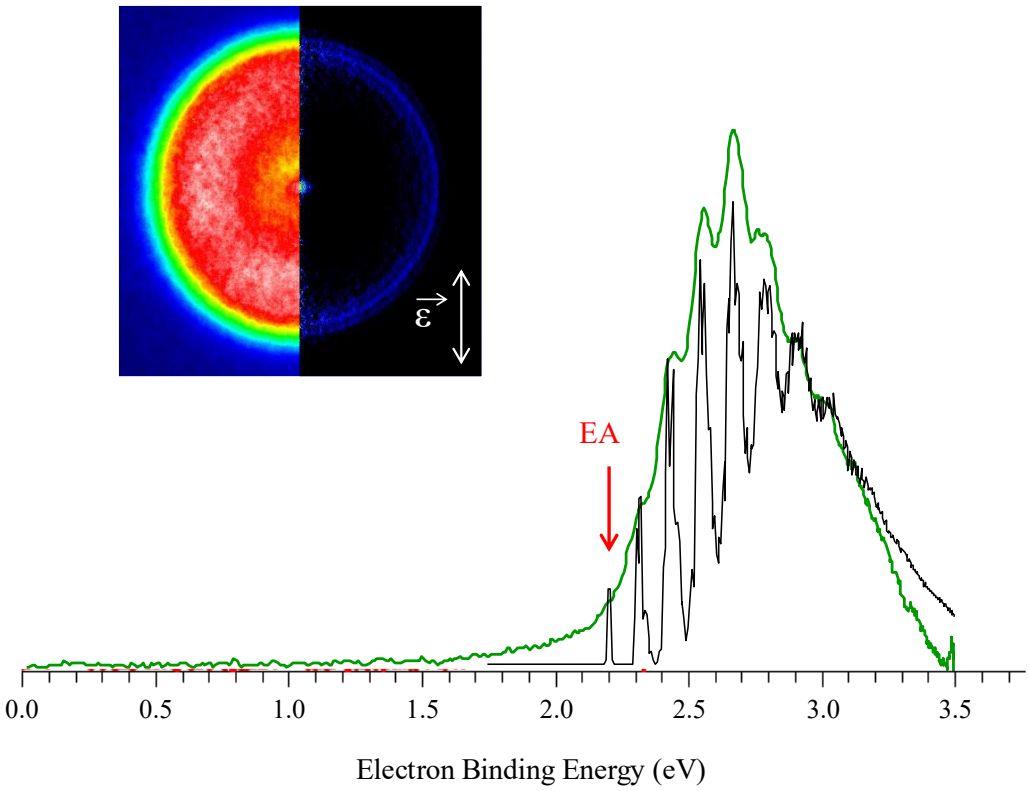

Figure 10: Photoelectron spectrum of oxazole made from the raw (left) and inverted Abel transformations (right) image on the left. The experimental spectrum is green, and the FC simulation is in black based on the frequencies using B3LYP level of theory with 6-31+G* basis set. The figure is based on data from reference 38.

5.1.3 – Isoxazole

The last molecule in this group is isoxazole (**5**). This is the five-membered ring within both anthranil and benzisoxazole. This molecule was studied by Wallace, et al.[39] where they found that all three carbons in the ring were deprotonated and contribute to the produced photoelectron spectrum. The spectrum was composed from images that were captured using 355 nm light from the Spectra Physics Nd:YAG laser with either O_2 or N_2O carrier gas. This experiment resulted in no clear vibrational progressions in the spectrum as it was congested with the presence of all three radical isomers. To identify where each isomer was, computations were done for theoretical EA and VDE values using EOM-IP-CCSD/aug-cc-pVTZ method. A σ and π isomer were determined for each deprotonation site, but within the range of the 355 nm spectrum shown in Figure 11, only 4 isomers are noted. These include both isomers at C5, the C4 σ state, and the C3 π state. These values are shown in the figure below, the boxes represent the EA on the left most side and the VDE on the right. The electron affinities for the three states that are worth noting here are: π(C3) at 2.96 eV, π(C5) at 3.33 eV, and σ(C5) at 2.46 eV.

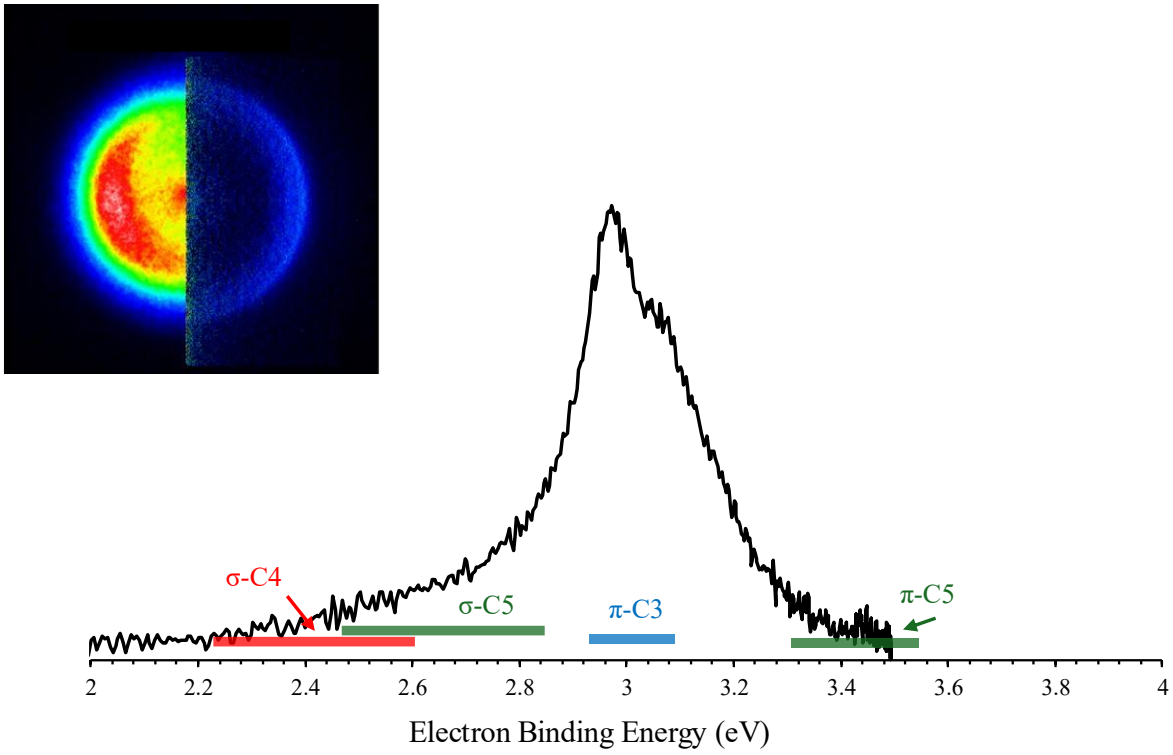

Figure 11: Photoelectron spectrum of isoxazole made by the images to the left obtained at 355 nm. The rectangles identify the range of each isomer's energies with the left end is the EA and the right end is the VDE value. The figure is based on data from reference 39.

5.2 – Bicyclic molecule to bicyclic molecule

After completing the analysis of the new molecules, a comprehensive comparison of the entire family can be made. The comparisons will focus on the C-H bond location in the molecules and the respective adiabatic electron affinities.

5.2.1 – Deprotonated carbon locations

First, the three bicyclic molecules will be compared with respect to the location of the deprotonated C-H bond. The bicyclic spectra were made from C2-benzoxazolyl, C3-anthranilyl and C3-benzisoxazolyl, respectively. These carbons are in the five-membered rings, between or next to the heteroatoms. Figure 12 presents the three photoelectron spectra overlapping each other.

When comparing the EA for benzoxazole and anthranil, considering the σ-radical only, it requires about 0.6 eV less to remove the hydrogen from benzoxazole relative to anthranil due to the proximity of the deprotonated carbon to the electronegative atoms. In benzoxazole, the C-H bond is between the nitrogen and oxygen atom, causing the electronegativity of those heteroatoms to create ease in deprotonation. The C3 in anthranil is next to the oxygen atom and a carbon binding the two rings together, so this bond would see an effect from the oxygen atom only.

When the heteroatoms move to form benzisoxazole, the EA shifts between its isomers. This respective carbon within benzisoxazole is similar to the location in anthranil but it is next to the nitrogen atom. Simply put, this carbon would feel less effects of the electronegativity than the carbon in anthranil, which means that it should have a lower EA.[11] This is supported by the theoretical values, with respect to the lowest lying isomers as benzisoxazolyl is around 2.94 eV

while anthranilyl is at 3.12 eV. It would require more energy than in benzoxazole because it is only near one heteroatom, not both, supporting the approximate 0.2 eV increase in electron affinities.

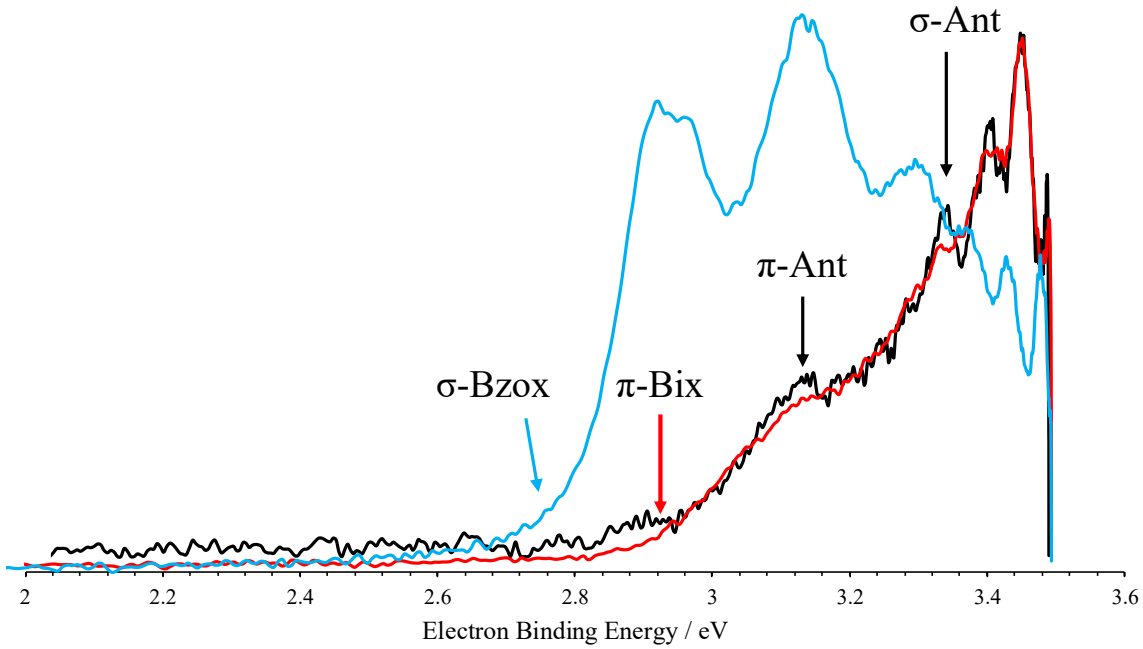

Figure 12: Photoelectron spectra produced from images captured at 355 nm of benzoxazole (blue), anthranil (black), and 1,2-benzisoxazole (red) layered on top of each other.

5.2.2 – Benzoxazole vs. Anthranil

Diving deeper into the behaviors of radicals, the deprotonation of C2-benzoxazole can result in a ring-open molecule from the cleaving of the C2-O bond within the five-membered ring. Breaking this bond causes the molecule to rehybridize and stabilize the π radical state, leaving the ring-open anion more stable than the ring closed geometry. This supports the idea that the rehybridization of benzoxazole is aided by the benzene ring unlike how the six-member ring in anthranil is unaffected in its π state. The aromaticity is focused within the benzene ring in benzoxazole while in anthranil, it is focused in the isoxazole ring. Therefore, the conjugation in benzoxazole happens within the benzene ring, changing its bonds so the C-O bond can become a double bond to stabilize the molecule. These changes do not happen when a A″ electron is removed in anthranil. In anthranil, the stabilization is reflected in the order of the energy levels, with the π sitting at the lower energy value. This occurs due to the oxygen being readily able to share its electrons. While there is not a ring open confirmation for anthranil, the lengthening of the N-O bond points to the possibility of the bond breaking.

5.2.3 – Benzisoxazole vs. Benzoxazole

When comparing benzoxazole and 1,2-benzisoxazole, one major similarity is the possible opening of the ring when in the anion form. In benzoxazole, the ring-open anion was possible, but it fell too closely to the closed ring anion to resolve as a separate peak in the spectrum. This resulted in the spectrum being composed solely of the σ radical. For benzisoxazole, the ring open conformation is the main anion form, yet this is not represented in the spectrum. The ring-open anion for benzoxazole was calculated at 2.66 eV and the benzisoxazole π radical is at 2.94 eV. The possibility of ring-open forms reflects the similarity between these molecules and highlights a difference from anthranil.

5.2.4 – Anthranil vs. 1,2-Benzisoxazole

When comparing these two benzisoxazoles, several elements need to be considered. In anthranil, the aromaticity of the molecule is centered within the five-membered ring, where as in benzisxoazole, it is focused within the benzene ring.[3, 10] Therefore, the five-membered ring is slightly less stable in the 1,2- orientation. This instability is what leads benzisoxazole to become ring-open at the lowest energy state while anthranil has the ring-closed σ state and π state within the spectral range. These two spectra are nearly identical, but the anthranil spectrum is easily understood after utilizing computation.

It is also worth noting that both states of anthranil are at a higher EA than the single state of benzisoxazole that is estimated to appear within the energy bounds. The anthranil spectrum includes two clear isomers at 3.12 eV and 3.34 eV while benzisoxazole would theoretically only have the lowest lying π state around 2.94 eV. This difference in energy can be partially attributed to the neighboring atoms. The slight electronegativity difference between nitrogen and oxygen can support the increase in electron affinity. It is also due to the difference in aromaticity within the molecules and the apparent π-stabilization effect that benzene has in anthranil. These studies highlight how different these two molecules act after deprotonation, despite their physical similarities.

5.3 – Whole and parts comparisons

5.3.1 – Benzoxazole versus Oxazole

When comparing the bicyclic molecules to their respective five-membered rings, only benzoxazole will be compared to oxazole. The site of interest in oxazole is C2 which is the carbon between the oxygen and nitrogen atoms. This corresponds to the identical carbon location

in benzoxazole. When comparing the σ radical electron affinities, benzoxazole has a higher EA by 0.54 eV, as seen in Figure 13. This increase is likely due to the benzene ring stabilizing the charge that is created from photodetachment as the more stable the anion, the more energy required to form the respective neutral radical. When comparing the two values of EA-VDE, both have differences of 0.6 eV apart, meaning the geometric differences between the anions and neutral radicals are similar.

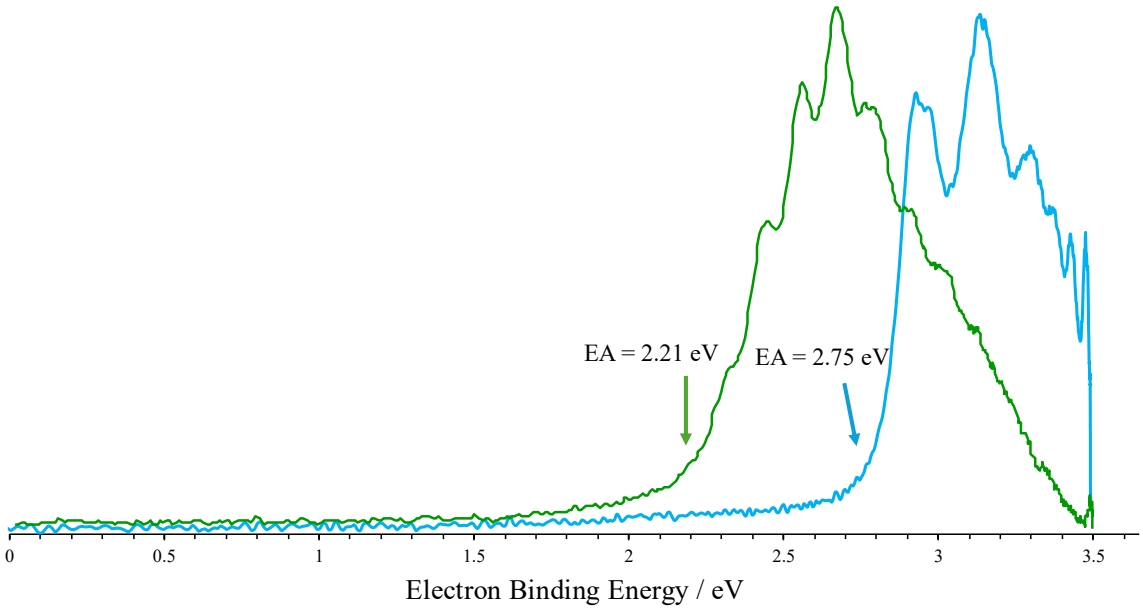

Figure 13: Overlapped photoelectron spectra made from the images obtained at 355 nm of benzoxazole (blue) and oxazole (green). The noted electron affinities are for the lowest lying σ state.

5.3.2 – Anthranil versus C5-Izoxazole

There is a similar trend seen when comparing anthranil to isoxazole. The carbon of interest in isoxazole for the comparison with anthranil is the C5 carbon. Since the study on isoxazole did not show clear separation between the isomers, calculations were utilized, resulting in all the locations having theoretical values for both the π (A″) and σ (A′) levels. The order of these levels switches in anthranil compared to isoxazole as shown in Figure 14. The π level is at a lower energy in anthranil due to the stabilizing effect that the benzene ring provides the deprotonated isomer which allows the π level to drop below the energy level of the σ isomer.[12] In addition, the stabilization from the benzene ring brings the energy levels, and the respective EAs, of anthranil closer together, compared to isoxazoles which have a spread of about 1.2 eV.

Another key difference when comparing these two molecules is that the experimental spectrum of isoxazole contains more than one isomer, making it difficult to clearly identify the individual isomers within the spectrum. This creates the need for theoretical analysis of each carbon around the ring. For anthranil, the spectrum is made from the deprotonated carbon near the heteroatoms with no contributions from the other C-H sites. Both molecules have π and σ radicals within the discernable spectral region. The radicals within the anthranil spectrum have different, separated peaks, highlighting another effect that benzene has on the molecule. The carbons around the six-membered ring allow for the C3 to stand out energetically.

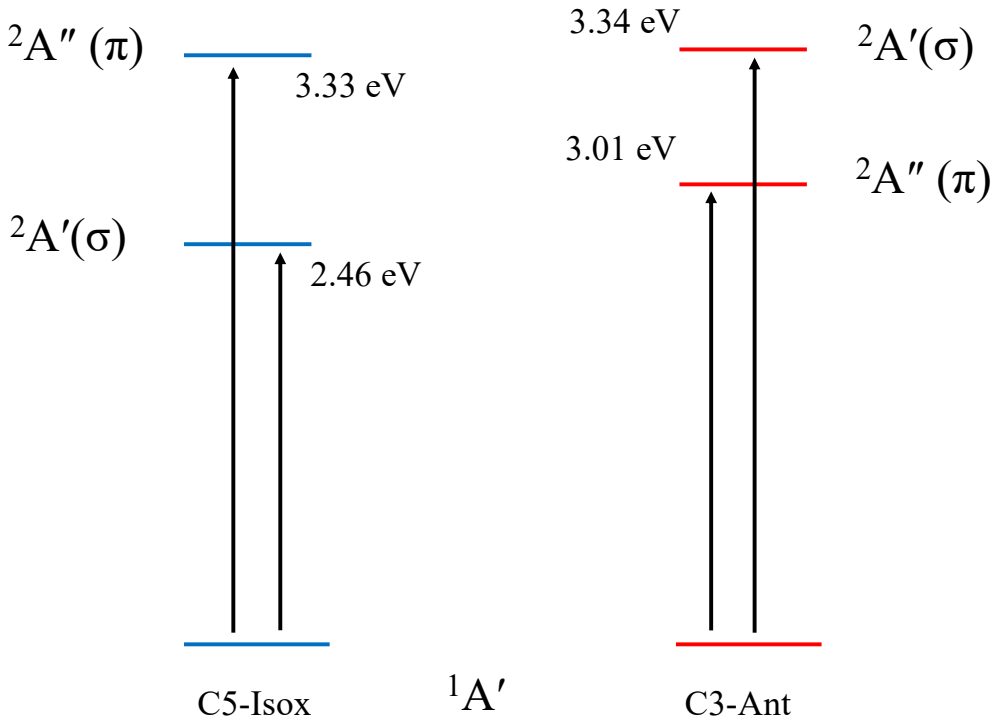

Figure 14: Energy diagram of the theoretical EA values for the π and σ isomers in C5-isoxazolide and C5-anthranide calculated at the CCSD level of theory with the aug-cc-pVDZ or TZ basis set.

5.3.3 – Benzisoxazole versus C3-Isoxazole

When comparing 1,2-benzisoxazole and isoxazole, the primary comparison location in isoxazole is C3. This location was seen to result in C3-enolate, similar as to how benzisoxazole opens when optimized. Since this C-H site is the same in both molecules, it can be expected that they would react the same, even with the addition of the benzene ring. The order of the energy levels for both molecules does not change, unlike in the previous comparison but here the π level is lower than the σ level. This is due to the significant similarities between these molecules, as the most stable confirmation is ring-opened for both molecules. The electron affinities are also very close in value as presented in Figure 15. The π levels are 0.02 eV higher in isoxazole and the σ is 0.04 eV lower. This slight change demonstrates that the π level is supported by the benzene although not significantly.

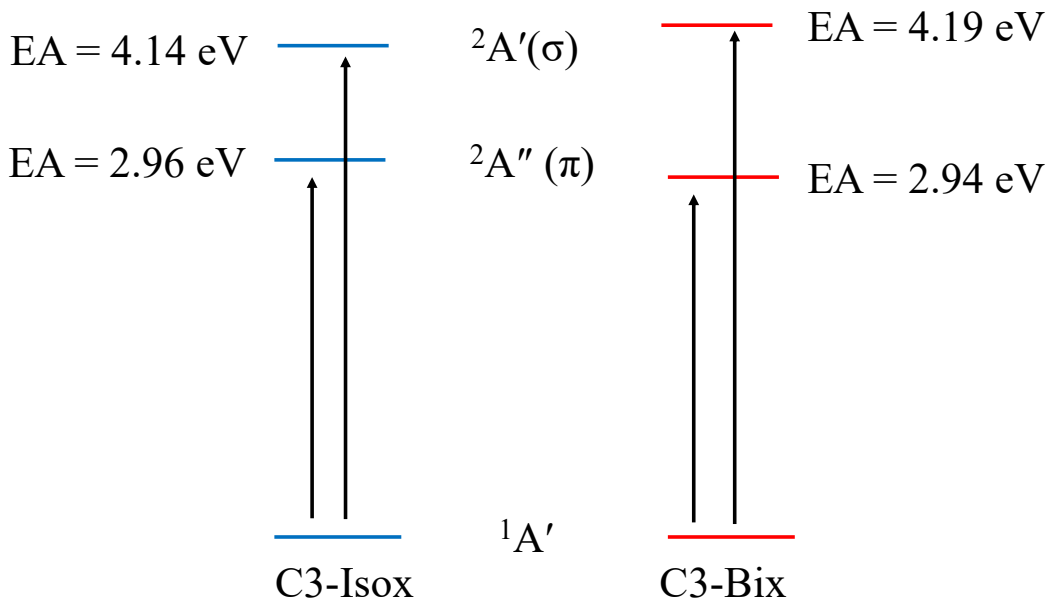

Figure 15: Energy diagram (not to scale) of the theoretical electron affinities of C3-isoxazolide and C3-benzisoxazolide calculated using EOM-IP-CCSD/aug-cc-pVTZ or DZ levels of theory showing the similarities in value.

Chapter 6: Summary

In this thesis, we used photoelectron spectroscopy to study bicyclic organic molecules and measure the adiabatic electron affinities of their radicals. The studies here are focused on experiments done at 355 nm light from Nd:YAG laser systems. The data presented for anthranil and 1,2-benzisoxazole show that the two isomers behave differently after being deprotonated. Anthranide results in π and σ radical states that appear as two distinct peaks within the photoelectron spectrum at 3.12 eV and 3.34 eV respectively. Benzisoxazole theoretically shows one π radical within the spectrum around 2.94 eV, but theoretical modeling of the peaks, used to identify elements within the spectrum, has proven inconclusive. The spectrum does not represent a ring-open molecule while computational results present optimized ring-open geometry.

These findings are compared to previously published work on the three other molecules within the isomer group. This creates the context for understanding the trends within the family of all five molecules based around the electron affinities and the influence of the heteroatoms. The results showed that anthranil has the largest EA within the bicyclic molecules, with both radicals being at greater energy values compared to its isomers. The C-H bond that is deprotonated is next to the nitrogen atom, the less electronegative of the two heteroatoms in the molecules. It is also the one molecule that sees π-stabilization effects due to the benzene ring, allowing the π radical to be at a lower energy than the σ radical. The molecule with the lowest EA is benzoxazole where the C-H bond is in between both the oxygen and nitrogen atom, creating an environment that sees the greatest electronegative effects.

When these molecules get put into context with their respective five-member ring elements, other trends are identified. Benzoxazole has a larger EA than oxazole by 0.54 eV, but the VDE values show that they experience similar geometric differences in the anion-radical

transition. With C5-isoxazole and anthranil, both radical forms are at a higher energy in anthranil and the order of the energy levels changes. Lastly, benzisoxazole and C3-isoxazole both result in optimized ring-open geometries as the N-O bond breaks. The EA for both the pi and sigma radicals in both molecules are nearly identical. This can reflect that the benzene ring does not have heavy effects on the radical states and that the two molecules behave the most similar out of the molecule group.

References:

(1) Bauer, M. R.; Di Fruscia, P.; Lucas, S. C. C.; Michaelides, I. N.; Nelson, J. E.; Storer, R. I.; Whitehurst, B. C. Put a ring on it: application of small aliphatic rings in medicinal chemistry. *RSC Medicinal Chemistry* **2021**, *12* (4), 448-471, 10.1039/D0MD00370K. DOI: 10.1039/D0MD00370K.

(2) Cordova, S.; Feng, B.; Fang, C.; Sanov, A. Photoelectron Spectroscopy and Ion Chemistry of Benzoxazolide. *J. Phys. Chem. Lett.* **2025**, *16* (22), 5546-5552. DOI: 10.1021/acs.jpclett.5c01067.

(3) Balaban, A. T.; Oniciu, D. C.; Katritzy, A. R. Aromaticity as a Cornerstone of Heterocyclic Chemistry. *Chem. Rev.* **2004**, *104* (5), 2777-2812.

(4) Alder, R. W. Medium-ring bicyclic compounds and intrabridgehead chemistry. *Accounts of Chemical Research* **1983**, *16* (9), 321-327. DOI: 10.1021/ar00093a002.

(5) Shastri, R. Review on synthesis of 3-substituted 1, 2-benzisoxazole derivatives. *Chem Sci Trans* **2016**, *5*, 8-20.

(6) Wong, X. K.; Yeong, K. Y. A Patent Review on the Current Developments of Benzoxazoles in Drug Discovery. *ChemMedChem* **2021**, *16* (21), 3237-3262. DOI: 10.1002/cmdc.202100370 From NLM Medline.

(7) Rakesh, K. P.; Shantharam, C. S.; Sridhara, M. B.; Manukumar, H. M.; Qin, H. L. Benzisoxazole: a privileged scaffold for medicinal chemistry. *Medchemcomm* **2017**, *8* (11), 2023-2039. DOI: 10.1039/c7md00449d From NLM PubMed-not-MEDLINE.

(8) Gao, Y.; Nie, J.; Huo, Y.; Hu, X.-Q. Anthranils: versatile building blocks in the construction of C–N bonds and N-heterocycles. *Organic Chemistry Frontiers* **2020**, *7* (9), 1177-1196. DOI: 10.1039/d0qo00163e.

(9) Serrano, J. L.; Soeiro, P. F.; Reis, M. A.; Boto, R. E. F.; Silvestre, S.; Almeida, P. Synthesis and process optimization of symmetric and unsymmetric barbiturates C5-coupled with 2,1-benzisoxazoles. *Mol Divers* **2020**, *24* (1), 155-166. DOI: 10.1007/s11030-019-09937-4 From NLM Medline.

(10) Domene, C.; Jenneskens, L. W.; Fowler, P. W. Aromaticity of anthranil and its isomers, 1,2-benzisoxazole and benzoxazole. *Tetrahedron Letters* **2005**, *46* (23), 4077-4080. DOI: 10.1016/j.tetlet.2005.04.014.

(11) Matos, M. Agostinha R.; Miranda, Margarida S.; Morais, Victor M. F.; Liebman, Joel F. Aspects of the Aromaticity of Anthranil. *European Journal of Organic Chemistry* **2004**, *2004* (15), 3340-3345. DOI: 10.1002/ejoc.200400158.

(12) Ming-Chiu Ou, S.-T. C. Pi-Electron Stablization in Benzocyclobutenes. *J. Phys. Chem.* **1993**, *98*, 1087-1089.

(13) Ashfold, M. N. R.; King, G. A.; Murdock, D.; Nix, M. G. D.; Oliver, T. A. A.; Sage, A. G. πσ* excited states in molecular photochemistry. *Phys. Chem. Chem. Phys.* **2010**, *12* (6), 1218-1238, 10.1039/B921706A. DOI: 10.1039/B921706A.

(14) Feng, B. Defying Limits: Electron Interactions with Atmospheric Species. *Ph.D. dissertation, University of Arizona, Tucson* **2023**.

(15) Surber, E.; Sanov, A. Photoelectron imaging spectroscopy of molecular and cluster anions: CS_2^- and $OCS^-(H_2O)_{1,2}$. *J. Chem. Phys.* **2002**, *116*, 5921-5924.

(16) Mabbs, R.; Surber, E.; Sanov, A. An experimental manifestation of distinct electronic-structural properties of covalent dimer anions of CO_2 and CS_2. *Chem. Phys. Lett.* **2003**, *381*, 479-485.

(17) Culberson, L. M. Molecular Electronic Structure via Photoelectron Imaging Spectroscopy. *Ph.D. dissertation, University of Arizona, Tucson* **2013**.

(18) Blackstone, C. C. Exploring the Chemistry of Methoxide with Oxygen Through Photoelectron Imaging Spectroscopy. *Ph.D. dissertation, University of Arizona, Tucson* **2020**.

(19) Wiley, W. C.; McLaren, I. H. Time-of-Flight Mass Spectrometer with Improved Resolution. *Rev. Sci. Instrum.* **1955**, *26* (12), 1150.

(20) Surber, E.; Ananthavel, S. P.; Sanov, A. Nonexistent electron affinity of OCS and the stabilization of carbonyl sulfide anions by gas phase hydration. *J. Chem. Phys.* **2002**, *116* (5), 1920-1929.

(21) Eppink, A. T. J. B.; Parker, D. H. Velocity map imaging of ions and electrons using electrostatic lenses: Application in photoelectron and photofragment ion imaging of molecular oxygen. *Rev. Sci. Instrum.* **1997**, *68* (9), 3477-3484.

(22) Dauletyarov, Y.; Wallace, A. A.; Blackstone, C. C.; Sanov, A. Photoelectron Spectroscopy of Biacetyl and Its Cluster Anions. *J. Phys. Chem. A* **2019**, *123* (19), 4158-4167. DOI: 10.1021/acs.jpca.9b01302.

(23) Mabbs, R.; Surber, E.; Sanov, A. Photoelectron Imaging of Negative Ions: Atomic Anions to Molecular Clusters. *Analyst* **2003**, *128* (6), 765-772.

(24) Feng, B.; Cordova, S.; Fang, C.; Sanov, A. Temporary Anions of Benzoxazole in Charge-Transfer Cluster Photodetachment. *The Journal of Physical Chemistry A* **2024**, *128* (40), 8717-8731. DOI: 10.1021/acs.jpca.4c05043.

(25) Dribinski, V.; Ossadtchi, A.; Mandelshtam, V. A.; Reisler, H. Reconstruction of abel-transformable images: The Gaussian basis-set expansion abel transform method. *Rev. Sci. Instrum.* **2002**, *73* (7), 2634-2642.

(26) Heck, A. J. R.; Chandler, D. W. Imaging Techniques For the Study of Chemical Reaction Dynamics. *Annu. Rev. Phys. Chem.* **1995**, *46*, 335-372.

(27) Shetnev, A.; Kotov, A.; Kunichkina, A.; Proskurina, I.; Baykov, S.; Korsakov, M.; Petzer, A.; Petzer, J. P. Monoamine oxidase inhibition properties of 2,1-benzisoxazole derivatives. *Mol Divers* **2024**, *28* (3), 1009-1021. DOI: 10.1007/s11030-023-10628-4 From NLM Medline.

(28) Yu, S.; Tang, G.; Li, Y.; Zhou, X.; Lan, Y.; Li, X. Anthranil: An Aminating Reagent Leading to Bifunctionality for Both C(sp(3))-H and C(sp(2))-H under Rhodium(III) Catalysis. *Angew Chem Int Ed Engl* **2016**, *55* (30), 8696-8700. DOI: 10.1002/anie.201602224 From NLM PubMed-not-MEDLINE.

(29) Krylov, A. I. Equation-of-motion coupled-cluster methods for open-shell and electronically excited species: The Hitchhiker's guide to Fock space. *Annu. Rev. Phys. Chem.* **2008**, *59*, 433-462. DOI: DOI 10.1146/annurev.physchem.59.032607.093602.

(30) Condon, E. A Theory of Intensity Distribution in Band Systems. *Phys. Rev.* **1926**, *28* (6), 1182-1201. DOI: 10.1103/PhysRev.28.1182.

(31) Condon, E. U. The Franck-Condon Principle and Related Topics. *Am. J. Phys.* **1947**, *15* (5), 365-374. DOI: 10.1119/1.1990977.

(32) Franck, J.; Dymond, E. G. Elementary processes of photochemical reactions. *Trans. Faraday Soc.* **1926**, *21* (February), 536-542, 10.1039/TF9262100536. DOI: 10.1039/TF9262100536.

(33) Epifanovsky, E.; Gilbert, A. T. B.; Feng, X.; Lee, J.; Mao, Y.; Mardirossian, N.; Pokhilko, P.; White, A. F.; Coons, M. P.; Dempwolff, A. L.; et al. Software for the frontiers of quantum chemistry: An overview of developments in the Q-Chem 5 package. *J. Chem. Phys.* **2021**, *155* (8), 084801. DOI: 10.1063/5.0055522 (acccessed 8/22/2024).

(34) Duschinsky, F. The importance of the electron spectrum in multi atomic molecules. Concerning the Franck-Condon principle. *Acta Physicochim. URSS* **1937**, *7* (4), 551-566.

(35) Kabi, A. K.; Gujjarappa, R.; Garg, A.; Sahoo, A.; Roy, A.; Gupta, S.; Malakar, C. C. Overview on Diverse Biological Activities of Benzisoxazole Derivatives. Singapore, 2022; Springer Nature Singapore: pp 81-98.

(36) Sah, C.; Yadav, A. K.; Venkataramani, S. Deciphering Stability of Five-Membered Heterocyclic Radicals: Balancing Act Between Delocalization and Ring Strain. *J. Phys. Chem. A* **2018**, *122* (24), 5464-5476. DOI: 10.1021/acs.jpca.8b03145.

(37) Casey, M. L.; Kemp, D. S.; Paul, K. G.; Cox, D. D. Physical organic chemistry of benzisoxazoles. I. Mechanism of the base-catalyzed decomposition of benzisoxazoles. *The Journal of Organic Chemistry* **1973**, *38* (13), 2294-2301. DOI: 10.1021/jo00953a006.

(38) Culberson, L. M.; Blackstone, C. C.; Wysocki, R.; Sanov, A. Selective deprotonation of oxazole and photoelectron imaging of the oxazolide anion. *Phys. Chem. Chem. Phys.* **2014**, *16* (2), 527-532, Article. DOI: 10.1039/c3cp53176g.

(39) Wallace, A. A.; Dauletyarov, Y.; Sanov, A. Deprotonation of Isoxazole: A Photoelectron Imaging Study. *J. Phys. Chem. A* **2020**, *124* (38), 7768-7775. DOI: 10.1021/acs.jpca.0c06838.